

On the synergistic effects of helium and hydrogen in bubble formations and materials degradation

Sangeun Kim^a, Hyeongchul Kim^a, Jinhyeok Kim^a, Chansun Shin^a, Hyung-Ha Jin^b, Joonoh Moon^c, Chang-Hoon Lee^c

^aDepartment of Materials Science and Engineering, Myongji University

^bNuclear Materials Safety Research Division, Korea Atomic Energy Research Institute(KAERI)

^cFerrous Alloy Department, Korea Institute of Materials Science (KIMS)

*Corresponding author: c.shin@mju.ac.kr

1. Introduction

Cavities (voids and helium bubbles) can form in metals, which are subjected to neutron irradiation, by the agglomeration of vacancies produced by neutron bombardment and/or helium atoms generated by neutron-induced transmutation. The volumetric changes and degradation in mechanical properties because of swelling and cavities, respectively, have been of intense interest in nuclear applications [1]. One of the most studied materials is reduced activation ferritic martensitic (RAFM) steel, which is a candidate structural materials for use in the blankets of fusion reactors. RAFM steels will be exposed to high temperature and neutron irradiation. Helium and hydrogen atoms are generated through nuclear interactions of host atoms with the incident neutrons via (n, α) and (n, p) reactions [2].

In this study, we present the surface swelling induced by helium implantation for RAFM steels with and without pre-implanted hydrogen. Regular surface patterns with a step height of a few tens of nanometers and enhanced hardness are generated by masking the surface of RAFM steels with a square mesh transmission electron microscopy (TEM) grid during helium implantation. The cause of the difference in surface-step heights is evaluated using cross-sectional TEM observation and attributed to the change in microstructural features in the steels. Pre-implantation of hydrogen enhances the surface swelling with only one-twentieth dose of post-implanted helium ions. Possible mechanisms are postulated in this study to explain the synergistic effect of pre-implanted hydrogen.

2. Experimental

The composition of RAFM steel used in this study is Fe-0.092C-8.83Cr-1.02W-0.435Mn-0.214V-0.133Si-0.089Ta-0.014Ti (in wt.%). The alloy was normalized at 1000 °C for 30 min, followed by water quenching. Normalized steel was then tempered at 750 for 90 min and then air-cooled.

200-keV He ions were implanted on the polished samples of RAFM steel with a dose of 0.5×10^{17} and 1×10^{17} ions/cm² in a vacuum chamber at room temperature. Helium was implanted using ion-beam accelerators at the Korea multi-purpose accelerator

complex. A TEM grid with 50 μm opening size was attached to the surface of each polished sample before ion implantation to form selective helium-implanted regions through TEM-grid holes as displayed in Fig. 1(a). The depth profile of He ion distribution is displayed in Fig. 1(b) as calculated using SRIM simulations [3] for a dose of 1×10^{17} ions/cm². Another He-ion implantation with 1×10^{17} ions/cm² was performed on the samples pre-implanted with 3-MeV H ions with 0.05×10^{17} ions/cm². The calculated distributions of damage in displacement per atom (dpa) and H-ion concentration are also displayed in Fig. 1(b). The helium-implanted samples were annealed for 2 h at 350 °C in an argon atmosphere after detaching the TEM grid. Subsequently, the surface swelling was measured by a contactless 3D surface profiler (NV2700, NanoSystem, Korea) that has a vertical resolution of 0.1 nm using white-light scanning and phase-shift interferometry.

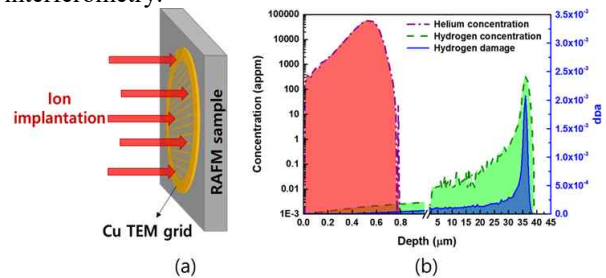


Fig. 1. (a) Schematic diagram of helium ion implantation on TEM-grid-covered sample, (b) depth-dependent damage and implanted ion concentration profiles calculated using SRIM code

3. Results and discussion

Fig. 2(a) depicts the surface plateaus of the He-ion implanted RAFM steel measured after post-implantation annealing (PIA) by the 3D surface profiler. Aligned upheaved surface square-patterns corresponding to TEM-grid meshes are clearly visible. The step heights are measured from the surface profiles over at least 20 upheaved areas. Fig. 2(b) depicts the average step heights. The step height increases with the helium ion dose. By assuming that the swelling occurs along the vertical axis of the irradiation windows of a grid mesh, the swelling ($\Delta V/V$) can be calculated by dividing the

step height t by the helium penetration depth d , i.e., $\Delta V/V = (A \times t)/(A \times h) = t/h$, where A is the area of a TEM grid opening. The calculated swelling percentages are presented in Fig. 2(b) with the helium penetration depth of ~ 800 nm determined from Fig. 1(b).

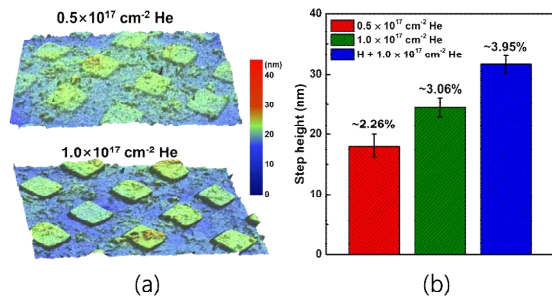


Fig. 2 (a) 3D optical profilometer images of helium implanted and post-implantation annealed RAFM, (b) average surface step heights and overall swelling (%) of the RAFM steel under various implantation conditions

Pre-implanted hydrogen atoms increase the step height significantly, as depicted in Fig. 4(b). The synergistic effects of pre-implanted hydrogen on the swelling of the subsequent helium implantation have previously been reported not only for RAFM steels [4,5] but also for other material [6]. The role of hydrogen or helium implantation in the pre-implanted helium or hydrogen layer is reported to be different, and a more pronounced swelling is observed for the He/H sequential condition than the H/He sequential condition [4, 6]. In the referred works, the synergistic effects were studied under implantation conditions such that helium and hydrogen have a similar projected range by applying a lower ion-acceleration energy for hydrogen. The H:He fluence ratio is set to $\sim 4:1$ to simulate the ratio of transmuted H and He production under fusion reactor conditions (14-MeV neutron irradiation). The synergistic effect observed in the present study, however, is surprising because the H:He fluence ratio is 1:20 and the projected ranges are ~ 36.5 and ~ 0.54 μm for hydrogen and helium, respectively.

The mechanism for the impacts of pre-implanted hydrogen is not clear, but dislocation loops induced by pre-implanted hydrogen are proposed to act as trap sites and help the nucleation of helium bubbles during subsequent helium implantation [4]. The vacancies introduced by pre-implanted hydrogen may enhance the nucleation of helium bubbles [6]. Hydrogen atoms decorating the outside of a helium bubble may impact the binding energies of He, vacancies (V), and self-interstitials, and increase the bubble size [7]. These explanations, however, are not applicable to the synergistic effect observed in this study because negligible ion-induced radiation defects and vacancies are generated along with negligible implanted hydrogen ions in the projected range of subsequent helium ions, as depicted in Fig. 1(b).

The hydrogen pre-implantation induces very low displacement damage (~ 0.002 dpa at the peak) and hence very low vacancies. Pre-implanted hydrogen forms loosely bound H_mV_n ($m > n$) and isolated H atoms at a depth of ~ 36.5 μm from the surface. Subsequent helium implantation forms V, V_n , He, He_m , and He_mV_n in the range of ~ 0.54 μm without any interaction with pre-formed hydrogen-related defects. Upon PIA, hydrogen atoms de-trapped from the traps and dissociated from H_mV_n diffuse toward the surface and inside the material. The calculated diffusion length at 350 $^\circ\text{C}$ for 2 h is ~ 10 nm for hydrogen using the lattice diffusivity data provided in [8]. Hence, hydrogen can interact with helium-related defects (He_mV_n) that are generated near the surface.

4. Conclusion

Pre-implantation of a small amount of hydrogen ions (H-to-He ratio ~ 0.05) is found to impact the amount of surface swelling significantly although the projected ranges of H (~ 36.5 μm) and He (~ 0.54 μm) are largely different. The synergistic effect on surface swelling is proposed to occur because of the diffusion of hydrogen atoms de-trapped from H-V complexes into the helium ion range where hydrogen atoms interact with small He_mV_n complexes to decelerate and increase the nucleation of embryonic bubbles.

REFERENCES

- [1] S.J. Zinkle, J.T. Busby, Structural materials for fission & fusion energy, *Materials Today*, Vol. 12, pp. 12-19, 2009.
- [2] J. Knaster, A. Moeslang, T. Muroga, *Materials research for fusion*, Nat. Phys., Vol. 12, pp.1-11, 2016.
- [3] J.F. Ziegler, J.P. Biersack, U. Littmark, *The stopping and Range of Ions in Solids*, Pergamon, New York, 1985.
- [4] W. Zhang, Z. Shen, Y. Long, Y. Wei, X. Zhou, C. Chen, L. Guo, J. Suo, Bubble-loop complexes induced by helium irradiation and effect of pre-irradiation and post-irradiation of hydrogen in reduced-activation ferritic/martensitic steel, *Phil. Mag.* Vol. 98, 2495-2511, 2018.
- [5] R. Ramachandran, C. David, P. Magudapathy, R. Rajaraman, R. Govindaraj, G. Amarendra, Study of defect complexes and their evolution with temperature in hydrogen and helium irradiated RAFM steel using positron annihilation spectroscopy, *Fusion Eng. Des.* Vol. 142, 55-62, 2019.
- [6] Z. Shen, Z. Zheng, F. Luo, W. Hu, W. Zhang, L. Guo, Y. Ren, Effects of sequential helium and hydrogen ion irradiation on the nucleation and evolution of bubbles in tungsten, *Fusion Eng. Des.* Vol. 115, 80-84, 2017.
- [7] E. Hayward, C. Deo, Synergistic effects in hydrogen-helium bubbles, *J. Phys.: Condens. Matter* Vol. 24, 265402, 2012.
- [8] M.A.A. Hasan, J. Wang, Y.C. Lim, A. Hu, S. Shin, Concentration dependence of hydrogen diffusion in α -iron from atomistic perspectives, *Int. J. Hydrog. Energy* Vol. 44, 27876-27884, 2019.